AIP | Applied Physics Letters

Isotopic tracing during rapid thermal growth of silicon oxynitride films on Si in O 2 , NH 3 , and N 2 O

I. J. R. Baumvol, F. C. Stedile, J.-J. Ganem, I. Trimaille, and S. Rigo

Citation: Applied Physics Letters **70**, 2007 (1997); doi: 10.1063/1.118804
View online: http://dx.doi.org/10.1063/1.118804
View Table of Contents: http://scitation.aip.org/content/aip/journal/apl/70/15?ver=pdfcov
Published by the AIP Publishing

Isotopic tracing during rapid thermal growth of silicon oxynitride films on Si in O_2, NH_3, and N_2O

I. J. R. Baumvol[a)]
Instituto de Fisica–UFRGS, 91540-000 Porto Alegre, RS, Brazil

F. C. Stedile
Instituto de Quimica–UFRGS, 91540-000 Porto Alegre, RS, Brazil

J.-J. Ganem, I. Trimaille, and S. Rigo
Groupe de Physique des Solides, URA 17–CNRS, Universités Paris 6 et Paris 7, Paris 75251, France

(Received 25 November 1996; accepted for publication 11 February 1997)

We performed isotopic tracing of O, N, and H during rapid thermal growth of silicon oxynitride films on silicon in two different sequential, synergistic gas environments: O_2, followed by NH_3, then followed by N_2O; and N_2O, followed by NH_3. Using nuclear reaction analysis and high resolution depth profiling, we demonstrate that the oxynitride films grow by means of thermally activated atomic transport involving the three traced species. Concomitantly, isotopic exchange processes take place. Growth in these sequential gas environments leads to oxynitride films with N concentration profiles and H concentrations different from those obtained by commonly used processes like thermal growth in N_2O only or thermal nitridation of SiO_2 films in NH_3. © *1997 American Institute of Physics.* [S0003-6951(97)03415-3]

Ultrathin films of silicon oxynitride on Si for gate dielectrics can be obtained by among other possibilities, direct thermal growth in N_2O or by thermal nitridation of SiO_2 films in NH_3. Thermal oxides nitrided in NH_3 show superior boron-stopping properties as compared to pure oxides, due to their incorporated N. However, these dielectric films suffer from H related electron trapping, either due to H atoms passivating the dangling bonds at the SiO_2/Si interface or due to Si–N–H bonds near this interface. On the other hand, oxynitride films grown in N_2O have shown superior electrical properties and reliability,[1–6] although presenting poorer boron-stopping properties due to the lower level of N incorporation. Furthermore, hydrogen exhibits a strong isotope effect in defect generation, as shown by recent studies in which transistors lifetime improvements (due to reduced interface states generation and hot-electron degradation) by factors of 10–50 were attained when hydrogen (H_2) was replaced by deuterium (D_2) in the final wafer sintering process.[5] These recent findings may help to understand further improvements in device performance that can be achieved when gate dielectrics are prepared by synergistic combinations of the above mentioned growth procedures.[7–11]

We report here to the best of our knowledge, on the first studies of isotopic tracing of N, O, and H during thermal growth of oxynitride films in a RTP furnace in the synergistic gas sequences reported in Refs. 7–11, namely (i) growth of a SiO_2 film in O_2, followed by nitridation in NH_3, and then followed by reoxynitridation in N_2O($O_2 \rightarrow NH_3 \rightarrow N_2O$, samples 1–5 in Table I),[7–9] and (ii) growth of oxynitride films in N_2O, followed by renitridation in NH_3($N_2O \rightarrow NH_3$, samples 6–8).[10,11] Isotopically enriched gases were used for the RTP growth, namely, 99% ^{18}O-enriched oxygen ($^{18}O_2$), 99.2% ^{15}N-enriched ammonia ($^{15}NH_3$) and nitrous oxide ($^{15}N_2O$), electronically pure N_2O containing N, O, and H isotopes in their natural abundancy ($^{14}N_2O$), and 99.7% ^2H-enriched ammonia ($^{14}N^2H_3$ or ND_3). The different sequences of isotopic gases and RTP parameters are given in Table I, together with the total amounts of all isotopes present in the resulting oxynitride films as measured by nuclear reaction analyses (NRA).[12] Since the overall N concentrations in most of the films are rather moderate, their density can be taken as being approximately that of vitreous silica, giving the equivalent thickness relationship 10^{15} (O+N) atoms/cm^2=0.226 nm. The ^{15}N and ^{18}O depth profiles were obtained by nuclear resonance profiling (NRP), using the strong, narrow, isolated resonances in the cross sections of the nuclear reactions $^{18}O(p,\alpha)^{15}N$ at 151 keV, and $^{15}N(p,\alpha\gamma)^{12}C$ at 429 keV, and a tilted sample geometry ($\Psi=65°$).[12–15] The measured excitation curves (i.e., α or γ yields versus incident proton energy) around the resonance energy E_R can be converted into concentration versus depth profiles by means of the SPACES simulation program.[12] This profiling method assures a depth resolution of approximately 1 nm near the film surface.

The excitation curves of the $^{18}O(p,\alpha)^{15}N$ nuclear reaction in samples 1–3 and the corresponding ^{18}O concentration ($^{18}O=[^{18}O]/[^{18}O]+[^{16}O]$) depth profiles are shown in Fig.

TABLE I. Total amounts of the isotopes in the oxynitride films grown by rapid thermal processing in different gas sequences. The rapid thermal processing parameters were in $^{18}O_2$, 1000 °C, 60 mbar, 60 s; in $^{15}NH_3$ and $^{14}N^2H_3$, 1000 °C, 100 mbar, 60 s; and in $^{14}N_2O$ and $^{15}N_2O$, 1100 °C, 30 mbar, 60 s. The errors in the total amounts of ^{16}O and ^{14}N are 10% and in the total amounts of ^{18}O, ^{15}N, and ^2H are 5%.

Sample No.	Gas sequence	Isotope (10^{15}. cm^{-2})				
		^{18}O	^{16}O	^{15}N	^{14}N	^2H
1	$^{18}O_2$	46.42	3.3	-	-	-
2	$^{18}O_2 \rightarrow ^{15}NH_3$	39.17	3.6	8.24	-	-
3	$^{18}O_2 \rightarrow ^{15}NH_3 \rightarrow ^{14}N_2O$	26.69	53.5	1.64	0.7	-
4	$^{18}O_2 \rightarrow ^{14}N^2H_3$	40.73	4.1	-	7.7	0.70
5	$^{18}O_2 \rightarrow ^{14}N^2H_3 \rightarrow ^{15}N_2O$	27.85	52.9	0.66	1.9	0.08
6	$^{15}N_2O$	-	53.4	1.50	-	-
7	$^{14}N_2O \rightarrow ^{15}NH_3$	-	49.6	6.71	1.3	-
8	$^{15}N_2O \rightarrow ^{14}N^2H_3$	-	46.7	1.13	6.2	0.21

[a)] Electronic mail: israel@if.ufrgs.br

1. The ^{18}O profiles for samples 4 and 5 are identical to those for samples 2 and 3, respectively. The excitation curves of the $^{15}N(p,\alpha\gamma)^{12}C$ nuclear reaction in samples 2, 3, and 5 are shown in Fig. 2(a), where the ^{15}N concentration ($^{15}N = [^{15}N]/[N]+[O]$ depth profile for sample No. 2 (nitridation in $^{15}NH_3$ of the $Si^{18}O_2$ film) is shown in the inset. The ^{15}N depth profiles for samples 3 and 5 are shown in Fig. 2(b). In view of the symmetry of samples 3 and 5 with respect to the two N isotopes, we can say that the ^{15}N profile in sample 5 corresponds to the ^{14}N profile for sample 3, and vice versa. So, samples 3 and 5 have identical nitrogen ($^{15}N+^{14}N$) profiles, which is also shown in Fig. 2(b). The loss of ^{18}O in sample 2 from the near surface, bulk, and from the near oxynitride/silicon interface regions, with respect to sample 1, is due to the fact that the thermal nitridation of SiO_2 films in NH_3 proceeds by an exchange of O atoms from the silica network for freshly arriving N atoms.[15] Figure 2(a) shows that ^{15}N is incorporated in these regions, and in amounts comparable to the ^{18}O loss (Table I). In sample 3 there is a much larger loss of ^{18}O from the whole oxynitride film as compared to sample 2 due to the exchange of ^{18}O atoms from the oxynitride film for ^{16}O atoms from the $^{14}N_2O$ gas.[14] Besides this exchange, ^{16}O is transported to the oxynitride/silicon interface thus promoting film growth.[16,17] The reoxynitridation in $^{14}N_2O$ (sample 3), removes most of the ^{15}N from the surface, transporting part of the ^{15}N atoms into the bulk of the oxynitride film and towards the new oxynitride/silicon interface at the same time as it introduces a small amount of ^{14}N atoms into the entire growing film. The transport of part of the ^{15}N atoms towards the new interface can be attributed to a site-to-site jump mechanism (interstitialcy or vacancy) of diffusion of nitrogeneous species.[17] The removal of N from the near surface regions of an oxynitride film treated by RTP only in N_2O was demonstrated to be due to N↔O exchanges that result from the reaction of atomic oxygen (O) and O_2.[16,17] It is worth noting that the reoxynitridation in N_2O of an oxynitride film (samples 3 and 5) carries out N↔O and O↔O exchanges appreciably larger than the reoxidation in O_2 of the same oxynitride film,[14,15] evidence of different defect networks involved in each case, as well as the relevant role of O.

The thermal nitridation of a SiO_2 film in ND_3 incorporates approximately 1.5% of deuterium in the resulting oxynitride film (Table I, sample 4). The incorporated D was shown to be distributed mainly in near surface and near interface regions.[18] The thermal reoxynitridation of this film in N_2O (sample 5) removes approximately 90% of the D existing in sample 4 as a consequence of the diffusion and desorption of H and H_2O (or D and D_2O).[18]

Oxynitride films grown by RTP in N_2O display a characteristic N profile, whereby N is concentrated (1%–4%) only in the near interface region.[2,16,17,19,20] The ^{15}N depth profile for a sample prepared in the same conditions as sample No. 6 was previously reported in Ref. 17. Figure 3 shows the depth profiles of ^{15}N for samples 7 and 8 and the total nitrogen ($^{15}N+^{14}N$) profile. We notice from Fig. 3 that the nitridation in $^{15}NH_3$ of an oxynitride film grown in $^{14}N_2O$ (sample 7) introduces a significant amount of ^{15}N in the surface and bulk regions of the film, which did not contain any measurable nitrogen before this nitridation step.[20]

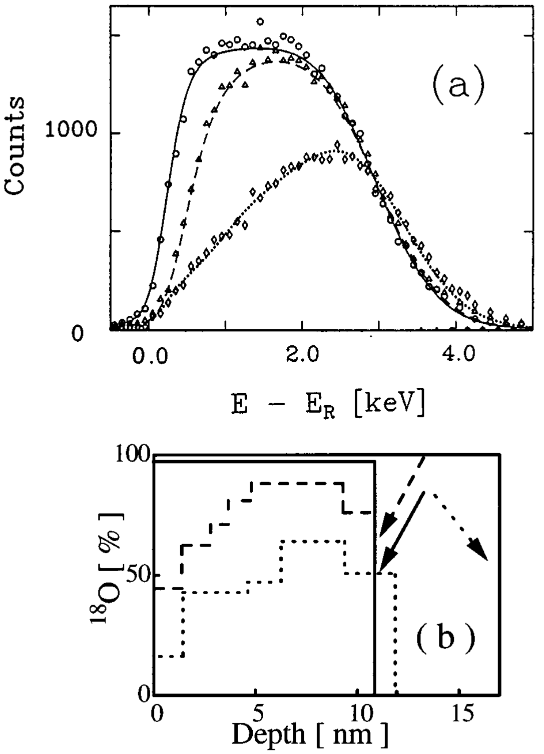

FIG. 1. (a) Excitation curves of the $^{18}O(p,\alpha)^{15}N$ nuclear reaction near the resonance at 151 keV, and the corresponding SPACES simulation curves, for a thermally grown $Si^{18}O_2$ film (sample 1, circle, solid line); for this oxide after thermal nitridation in $^{15}NH_3$ (sample 2 , triangle, dashed line); and for this oxide after thermal nitridation in $^{15}NH_3$, followed by reoxynitridation in $^{14}N_2O$ (sample 3, diamond, dotted line). (b) The corresponding ^{18}O depth profiles used for the SPACES simulation of the excitation curves. The arrows indicate the position of the oxide/Si or oxynitride/Si interfaces for each sample.

On the other hand, the nitridation in $^{14}ND_3$ of an oxynitride film grown in $^{15}N_2O$ (sample 8) shows that the ^{15}N atoms, which occupied only the near interface region before nitridation, are now also redistributed in the bulk and surface regions of the film, without major loss of ^{15}N. Furthermore, Table I shows that nitridation in ND_3 of an oxynitride film grown in $^{15}N_2O$ leads to the incorporation of D to a concentration smaller than that in sample 4, but much larger than that in sample 5.

In summary, the isotopic tracing results here reported show that the oxynitride films grow by means of atomic transport at the same time as atomic exchanges processes take place and lead to redistributions of the species constituting the films after each thermal treatment step. In the films thermally grown in the $O_2 \rightarrow NH_3 \rightarrow N_2O$ sequence, the main mechanisms taking place are (i) during nitridation in NH_3, the exchange of O for N atoms and the incorporation of H (D); and (ii) during reoxynitridation in N_2O, the exchange of O atoms from the film for those of the gas phase; the removal of N from the surface, the transport of an appreciable amount of N from the surface into the bulk and of a moderate amount of N towards the new interface; the removal of most of the H (D) atoms from the film; and the growth of the oxynitride film. For films thermally grown in

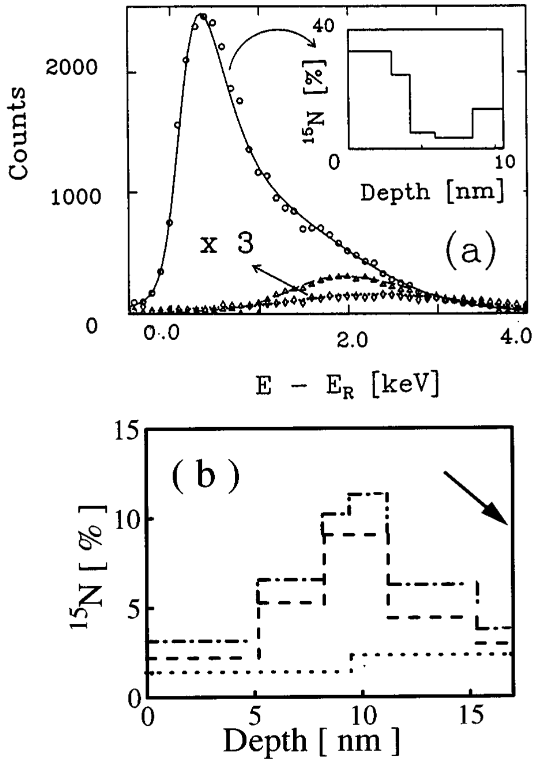

FIG. 2. (a) Excitation curves of the $^{15}N(p,\alpha\gamma)^{12}C$ nuclear reaction near the resonance at 429 keV, and the corresponding SPACES simulation curves, for the $Si^{18}O_2$ film of Fig. 1 after thermal treatments in $^{15}NH_3$ (sample 2, circle, solid line); $^{15}NH_3$ followed by $^{14}N_2O$ (sample 3, triangle, dashed line); and $^{14}ND_3$ followed by $^{15}N_2O$ (sample 5, diamond, dotted line). The ^{15}N depth profile of sample 2 is shown in the inset where the oxynitride/Si interface coincides with the end of the ^{15}N profile. (b) ^{15}N depth profiles for sample 3 (dashed line), and for sample 5 (dotted line). The total nitrogen ($^{14}N+^{15}N$) profile is also shown (dash-dotted line). The arrow indicates the position of the oxynitride/Si interface.

the $N_2O \rightarrow NH_3$ sequence, the N that was incorporated into the near interface region of the film in the N_2O step is redistributed during the NH_3 step, concomitant with the heavy incorporation of additional N in the near surface region of the film, and in smaller amounts in the bulk and interface regions. Moderate atomic exchanges and no film growth were observed in the $N_2O \rightarrow NH_3$ sequence, while H (D) is seen to be incorporated into the oxynitride films in the last step. Both thermal treatment sequences lead to N concentration profiles appreciably different from those obtained by thermal nitridation of SiO_2 films in NH_3 or by direct oxynitridation in N_2O. The H (D) concentrations in the films of the present work are appreciably smaller than those obtained by thermal nitridation of SiO_2 films in NH_3.

The different gas sequences used to grow silicon oxynitride films in the present work allowed us to tailor the concentrations and depth distributions of N and H (D). The high N concentrations in the surface and bulk regions seem necessary to afford the N loss during B diffusion towards the oxynitride/Si interface.[6] On the other hand, the N concentrations near the interface obtained here (between 3% and 5%) seem to fall into the optimum range[11] for reduced interface state generation and hot-electron traps. The control of the H (D) concentrations near the oxynitride/silicon interface, on the other hand, is an essential aspect by which to take advantage of the passivating effect on the electrical activity, an effect that is largely magnified[5] when H is substituted for D atoms.

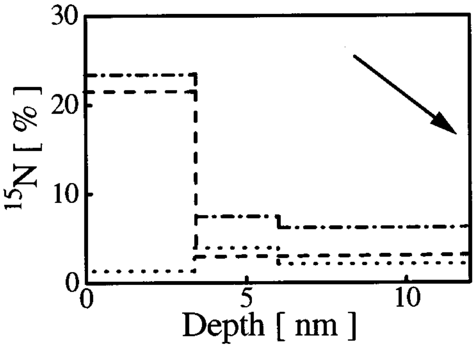

FIG. 3. ^{15}N depth profiles for oxynitride films thermally grown in $^{14}N_2O$ followed by $^{15}NH_3$ (sample 7, dashed line) and in $^{15}N_2O$ followed by $^{14}N^2H_3$ (sample 8, dotted line). The total nitrogen ($^{14}N+^{15}N$) profile is also shown (dash-dotted line). The arrow indicates the position of the oxynitride/Si interface.

This work was supported in part by the GDR86 of CNRS, France, and by CNPq and FAPERGS, Brazil.

[1] H. Fukuda, T. Endoh, and S. Nomura, in *The Physics and Chemistry of SiO_2 and the Si-SiO_2 Interface,* edited by H. Z. Massoud, E. H. Poindexter, and C. R. Helms (Eds.), Proceedings of The Electrochemical Society Vol. 96-1 Pennington, NJ, (1996), p. 15.
[2] Y. Okada, P. J. Tobin, V. Lakhotia, W. A. Feil, S. A. Ajuria, and R. I. Hedge Appl. Phys. Lett. **63**, 194 (1993).
[3] M. Bhat, J. Ahn, D. L. Kwong, M. Arendt, and J. M. White, Appl. Phys. Lett. **64**, 1168 (1994).
[4] D. Bouvet, P. A. Clivaz, M. Dutoit, C. Coluzza, J. Almeida, G. Margaritondo, and F. Pio, J. Appl. Phys. **79**, 7114 (1996).
[5] J. W. Lyding, K. Hess, and I. C. Kizilyalli, Appl. Phys. Lett. **68**, 2526 (1996).
[6] K. A. Ellis and R. A. Buhrman Appl. Phys. Lett. **69**, 535 (1996).
[7] L. K. Han, G. W. Yoon, J. Kim, J. Yan, and D. L. Kwong, IEEE Electron Device Lett. **16**, 348 (1995).
[8] T. Arakawa and H. Fukuda, Electron. Lett. **30**, 361 (1994).
[9] T. Arakawa, T. Hayashi, M. Ohno, R. Matsumoto, A. Uchiyama, and H. Fukuda, Jpn. J. Appl. Phys. 1 **34**, 1007 (1995).
[10] G. W. Yoon, A. B. Joshi, J. Kim, and D.-L. Kwong, IEEE Electron Device Lett. **14**, 179 (1993).
[11] M. Bhat, G. W. Yoon, J. Kim, D. L. Kwong, M. Arendt, and J. M. White, Appl. Phys. Lett. **64**, 2126 (1994).
[12] I. Vickridge and G. Amsel, Nucl. Instrum. Methods Phys. Res. B **45**, 6 (1990).
[13] I. J. R. Baumvol, F. C. Stedile, J.-J. Ganem, S. Rigo, and I. Trimaille, J. Electrochem. Soc. **142**, 1205 (1995).
[14] J.-J. Ganem, S. Rigo, I. Trimaille, I. J. R. Baumvol, and F. C. Stedile, Appl. Phys. Lett. **68**, 2366 (1996).
[15] I. J. R. Baumvol, F. C. Stedile, J.-J. Ganem, S. Rigo, and I. Trimaille, J. Electrochem. Soc. **143**, 2938 (1996).
[16] E. C. Carr, K. A. Ellis, and R. A. Buhrman, Appl. Phys. Lett. **66**, 1492 (1995).
[17] I. J. R. Baumvol, F. C. Stedile, J.-J. Ganem, S. Rigo, and I. Trimaille, Appl. Phys. Lett. **69**, 2385 (1996).
[18] I. J. R. Baumvol, F. C. Stedile, J.-J. Ganem, S. Rigo, and I. Trimaille, J. Electrochem. Soc. **143**, 1426 (1996).
[19] H.-T. Tang, W. N. Lennard, M. Zinke-Allmang, I. V. Mitchell, L. C. Feldman, M. L. Green, and D. Brasen, Appl. Phys. Lett. **64**, 3473 (1994); see also Nucl. Instrum. Methods Phys. Res. B **108**, 347 (1996).
[20] D. G. Shuterland, H. Akatsu, M. Copel, F. J. Himpsel, T. A. Callcot, J. A. Carlisle, D. L. Ederer, J. J. Jia, I. Jimenez, R. Perera, D. K. Shuh, L. J. Terminello, and W. M. Tong, J. Appl. Phys. **78**, 6761 (1995).